2021-07-01

Biochemical Impact of Solar Radiation Exposure on Human Keratinocytes Monitored by Raman Spectroscopy; Effects of Cell Culture Environment

Ulises Lopez Gonzalez
Technological University Dublin

Alan Casey
Technological University Dublin, alan.casey@tudublin.ie

Hugh Byrne
Technological University Dublin, hugh.byrne@tudublin.ie

Recommended Citation

Lopez-Gonzalez, U., Casey A. & Byrne, H.J. (2021) Biochemical impact of solar radiation exposure on human keratinocytes monitored by Raman spectroscopy; effects of cell culture environment,*Journal of Biophotonics,* 14, e202100058 (2021) DOI:10.1002/jbio.202100058

Funder: Consejo Nacional de Ciencias y Tecnologia (CONACYT), Mexico

Article type: Original Article

Biochemical impact of solar radiation exposure on human keratinocytes monitored by Raman spectroscopy; effects of cell culture environment

Ulises Lopez-Gonzalez*[1], Alan Casey[1], Hugh J. Byrne[2]

[1] School of Physics, Nanolab Research Center, FOCAS Research Institute, Technological University Dublin, Dublin 8, Ireland.
[2] FOCAS Research Institute, Technological University Dublin, Dublin 8, Ireland.

*Correspondence
Ulises Lopez-Gonzalez, FOCAS Research Institute, Technological University Dublin, Kevin street, Dublin 8, Ireland., Affiliation, Postcode City, Country
Email: uli.lg27@gmail.com

Abstract

Understanding and amelioration of the effects of solar radiation exposure are critical in preventing the occurrence of skin cancer. Towards this end, many studies have been conducted in 2D cell culture models under simplified and unrealistic conditions. 3D culture models better capture the complexity of in vivo physiology, although the effects of the 3D extracellular matrix have not been well studied. Monitoring the instantaneous and resultant cellular responses to exposure, and the influence of the 3D environment, could provide an enhanced understanding

of the fundamental processes of photocarcinogenesis. This work presents an analysis of the biochemical impacts of simulated solar radiation (SSR) occurring in immortalised human epithelial keratinocytes (HaCaT), in a 3D skin model, compared to 2D culture. Cell viability was monitored using the Alamar Blue colorometric assay (AB), and the impact of the radiation exposure, at the level of the biomolecular constituents (nucleic acids and proteins), were evaluated through the combination of Raman microspectroscopy and multivariate statistical analysis. The results suggest that SSR exposure induces alterations of the conformational structure of DNA as an immediate impact, whereas changes in the protein signature are primarily seen as a subsequent response.

Keywords: Principal Components Analysis, Partial Least Squares Regression, Raman spectroscopy, 3D Cell culture models, solar radiation,

Abbreviations: AB1, alamar blue 1; **SSR2,** simulated solar radiation 2; **ECM3**, extracellular matrix 3; **IR4,** Infrared spectroscopy 4; **PBS5**, phosphate buffered saline 5; **HDF6**, human dermal fibroblast 6; **PCA7**, principal components analysis 7; **PLSR8**, partial least squares regression 8; **EMSC9**, extended multivariate signal correction 9.

1 INTRODUCTION

Cell culture systems, both two-dimensional (2D) andthree-dimensional (3D) models, are invaluable tools com-monly employed to provide a better understanding of themechanisms that underlie in vivo cell behaviour [1]. Tra-ditionally, 2D cell cultures have been accepted and usedto study cellular responses to stimulations from biochem-ical and biophysical signals of the microenvironment [2].However, this practice of culturing cells on flat, syntheticand rigid substrates does not reproduce the in vivo cellu-lar microenvironment, leading to results that are ques-tionably representative of true cellular behaviour [1,3, 4]. As an alternative, 3D models

provide cells with anextracellular matrix (ECM) which allows cellular prolifer-ation, differentiation, mechano-responses and communi-cation [1, 2, 5]. A wide variety of biomaterials forsupporting and guiding 3D culture and tissue formationexists on the market. Scaffold type substrates can bederived from animal (Matrigel, Collagen) or plant (QGelMatrix, 3-D Life Biomimetic, Puramatrix) sources;whereas, scaffold-free options range from adhesionplates, hanging drop models, magnetic levitation tech-niques, and so forth [6–8]. Reconstructed artificialmodels of skin have been developed to mimic the 3Dorganisation of human skin [9, 10]. However, suchmodels present limitations in their barrier function, pri-marily presented by the outermost, stratum corneumlayer [11], limiting observations in the development ofthe responses to external stimuli, which is of interest infor example, studies of skin damage and toxicity.

In previous studies, it was shown that simulated solarradiation (SSR) exposure can produce short and long-term detrimental effects on keratinocytes (HaCaT)cultured in 2D models [12, 13]. The radiation and cellinteraction induces a series of immediate and later bio-chemical responses through the interaction with endo-genous photosensitizers, which can be translated in theformation of reactive oxygen and nitrogen species (ROSand RNS), single strand break, DNA-protein cross linksand the formation of cyclobutane pyrimidine dimers[12, 14, 15]. Such reactive species can be generated by radiation across the solar spectrum, highlighting theimportance of not only the UV wavelengths in the studyof the effects of solar radiation [16, 17]. Moreover, it isimportant to examine whether the environment of cellculture impacts on the observations of the effects of SSRon the cell characteristics, both in the short and long-term post exposure, and to understand any protectiveeffects that may be inferred by the ECM environment.

In a previous study of SSR of HaCaT, in addition to conventional cytotoxicity assay screening of cellular responses, Raman microspectroscopy was demonstrated to be an ideal technique to identify variations in cellularmetabolism as a result of the external insult [12, 18, 19].This

technique allows rapid, non-destructive and high spa-tial resolution measurements (~0.5–1.5μm) in tissues orsingle cells. The Raman spectra exhibit information aboutcellular components (e.g. proteins, lipids, nucleic acids) orspecific molecules in these groups (e.g. phenylalanine,amide I, adenine, cytosine, tyrosine) which can be alteredupon exposure to external stimuli such as solar radiation[12, 19–21]. Raman spectroscopy is relatively insensitive towater, compared to, for example, the complementary tech-nique of infrared absorption spectroscopy, and little or nosample preparation is required [22]

In this study are evaluated the effects of culturingHaCaT cells in a 3D microenvironment upon SSR expo-sure per different points in time. Raman spectroscopy,coupled with multivariate statistical analysis techniques,is employed as a powerful tool to investigate the immedi-ate and longer-term cell responses to solar radiation.Comparison of the spectral signatures of HaCaT cellsexposed to SSR in 2D and 3D models is explored to pro-vide information regarding the differences and similarities between the two cell culture systems under the same exposure conditions.

2 EXPERIMENTAL SECTION

2.1 Materials

Cell culture media, foetal bovine serum and trypsin were sourced from Sigma Aldrich Ltd. (Arklow, Co. Wicklow, Ireland). Collagen I Rat-Tail (Gibco)- LOT Number 1851583, Geltrex® hESC-qualified Ready-to-Use Reduced Growth Factor Basement Membrane Matrix, Catalogue Number A1569601, as well as Alamar Blue® (AB) were sourced from Biosciences (Dublin, Ireland). 35 mm glass bottom Petri dishes were obtained from MatTek Life for Science (Boston, USA). Phenol-red free cell culture media were purchased from Thermo Fisher Scientific (Dublin, Ireland).

2.2 HDF and HaCaT cell lines

Adult human dermal fibroblast (HDF) cells (106-05A) were obtained from Sigma Aldrich Ltd. (Arklow, Co. Wicklow, Ireland), and immortalised human dermal keratinocytes (HaCaT) from the Leibnitz Institute, DSMZ-German Collection of Microorganisms and Cell Cultures. Both were cultured in Dulbecco's Modified Eagle Medium: Nutrient Mixture F-12 (DMEM/F12) supplemented with 10% foetal bovine serum under standard conditions of 5% CO_2 at a temperature of 37 °C and humidity of 95%. [6] The cell cultures were maintained until they reached a confluency of approximately 80-90%. They were then detached by trypsin and seeded in co-culture, as described in section 2.5. All the experiments were performed in triplicates.

2.3 Co-culture model preparation

2.3.1 Collagen substrate preparation (dermal substrate)

Collagen I Rat Tail (Gibco) was utilised to replicate the ECM found in the dermis of the skin. In the substrate preparation, 3 mg/ml solution was mixed with 1 M sodium hydroxide (1 M NaOH), 10X phosphate buffered saline (PBS) and distilled water (dH_20). All constituents were previously sterilised. The relative quantities of these components are determined by the final concentration of 2.5 mg/ml and the volume required. [6] After mixing, 500 µl of the solution were placed into a 35 mm glass bottom Petri dish, before incubation at a temperature of 37 °C degrees in a 95% humidity incubator in 5% CO_2 conditions, until a solid gel was seen to form (45 – 60 min). All preparation steps were performed on ice to avoid premature gelation.

2.3.2 Geltrex substrate preparation

Geltrex was used to replicate the basement membrane found in the epidermis of the skin and it served as a base to seed keratinocytes cells on top of the co-culture system. Geltrex is a ready to use, reduced growth factor basement membrane matrix, which means no thawing or dilution is required. Similar to Matrigel, it is derived from the Engelbreth-Holm-Swarm tumour. [6] To

avoid gelation, the Geltrex stock was placed on ice and 200 µl of the solution were placed on top of each previously prepared collagen substrate. The samples were then incubated for ~1 h until the basement membranes were seen to form.

2.3.3 Co-culture preparation

Co-cultures were established by embedding $1x10^6$ HDF cells in a solid collagen and Geltrex covered substrate and then incubating for 24 hrs to form a dermal substrate. After that time, to replicate the epidermis of the skin, $1x10^5$ HaCaT cells were incorporated into the co-culture system. HaCaT cells were seeded on top of the dermal substrate and grown submerged in DMEM F-12 medium (2 ml) until they formed a complete layer (13 days). The co-culture model was monitored and the medium was changed every 2-3 days. Once the co-culture models were ready to use, they were exposed to simulated solar radiation and subjected to cell viability assessment, morphological examination by hematoxylin and eosin (H&E) staining and Raman spectroscopic analysis. All experiments were performed in triplicates, 3 Petri dishes for control and 3 for each exposure time point.

2.4 Dosimetry

o produce the damage caused by full-spectrum sunlightto cells, irradiation of the samples was performed using afull spectrum Q-sun solar simulator (Q-panel, Cleveland)[13, 23]. The instrument simulates exposure to the fullsolar spectrum, including UVA and UVB regions [13].Internal optical filters modify the lamp output to delivera spectrum which is equivalent to summer sunlight atnoon at the equator. The irradiance intensity at the sam-ple is specified by the user, and controlled by internalsensors. The instrument is routinely calibrated every~1000 hours. The integrated spectral distribution over therange 280 to 400 nm constitutes a total UV intensity of 63.63 Wm^{-2}, proportioned as 62.30 Wm^{-2} within 315-400 nm (UVA) and 1.33 Wm^{-2} in the range 280-315 nm (UVB). [12] The Q-sun simultaneously delivers~400 W m^2over the

range 400 to 700 nm [23]. In the NIR region, although a similar dose is delivered, it will be attenuated by the water immersion environment. In the presentation of the results, the exposures are given in terms of exposure time. These valeus can be easily converted to UV dose, noting that 1 W m^{-2} equals 1 J m^{-2} s^{-1}. [12]

2.5 Solar Exposure

In previous studies, Maguire et al.[24] reported death of keratinocytes after similar full specral SSR exposure due to the formation of ROS, via riboflavin photosensitisation and degradation within the in vitro cell culture medium. Therefore, in the current study, the culture medium was removed and exchanged for PBS, prior to exposure to SSR. In order to perform the irradiation exposure without plastic lids, ensuring exposure of the cells to the full simulated solar spectrum, the irradiation compartment of the Q-sun was sterilised with 100% methanol. The instrument was allowed to stabilise for 15 min after ignition. The temperature inside the chamber was set to 37 ºC. Samples were irradiated for varied periods of 30, 60, 90, 120 and 180 min. Little or no difference was reported by Maguire et al. in the cellular viability of controls which were maintained in the incubator, or removed and "sham irradiated" in the solar simulator.[24] Thus, control samples received the same treatment as the irradiated ones, except that they were kept in the incubator while the exposed samples underwent irradiation. Post exposure, the samples were removed from the Q-sun irradiation compartment and were split into two groups. The first group was used for immediate (taking into account sample preparation, approx. 10 min) assessment of cell viability, and Raman spectroscopic evaluation. Samples of the second group were returned to the incubator at 5% CO_2 and 37 °C before their further analysis, 24 hr post-exposure, after the PBS was removed and replaced by pre-warmed medium.

2.6 Light microscopy imaging

The co-culture model was fixed in 4% formaldehyde for 3 hrs. Then, the model was cut vertically, perpendicular to the surface of the sample, in 4 pieces, embedded in paraffin wax, and subsequently dewaxed. Cross-sectional samples of 10 μm thickness were microtomed, mounted on glass slides and then dried. The samples were dewaxed by immersion in a series of baths; two baths of xylene (Lennox, Dublin) for 5 and 4 min, respectively, two of absolute ethanol (Lennox, Dublin) for 3 and 2 min, and finally a bath of 95% Industrial Methylated spirits (Lennox, Dublin) for 1 min. The samples were then stained routinely using H&E, enabling visualisation of the general morphology of the co-culture model. All samples were cover slipped for microscopic observation (BX51 Olympus) at a magnification of 100× (Olympus MPLN, NA 0.9) and then photographed.

2.7 Cell viability measurement with Alamar Blue

The Alamar Blue (AB) assay is commonly employed as amethod to quantitatively assess cellular proliferation [18].Due to its sensitivity and non-toxic properties, this bioas-say is one of the preferred methods in analysis of meta-bolic function, cytotoxicity and in irradiation studies [7,25–27]. The AB assay acts as an indicator of the metabolic activity of cells by the reduction of the blue, non-fluorescent and cell membrane permeating reagent (Resazurin) to its pink, highly fluorescent state (Resorufin). [26] In this study, the colorometric AB reduction assay was conducted to elucidate the presence of live cells in the co-culture model, post exposure to SSR. The assay was performed for the first group, immediately after irradiation (within 10 min for sample preparation) and for the second, incubated for 24 h post-exposure. Unexposed co-culture models were included as controls in the experimental design. Post irradiation exposure, the PBS was removed from the samples, and they were incubated in AB solution (3 ml of 5% [v/v] solution of AB dye) prepared in un-supplemented (no FBS) medium which was pre-warmed, and subsequently incubated at 37 °C, 5% CO_2 for 3 h. As a measure of the metabolic activity of cells, AB conversion was determined using a spectroscopic plate

reader (SpectraMax—M3) to monitor the fluorescence, excited by 540 nm and emitted at 590 nm.

2.8 Raman Spectroscopy

This work employed a Horiba Jobin-Yvon LabRAMHR800 spectrometer, with a 16-bit dynamic range Peltier cooled CCD detector. It has an external 300 mW 785 nm diode laser as source, producing ~70 mW at the sample. For the measurements, an Olympus LMPLFLNx100immersion objective (NA 0.8) was employed, resulting in a spatial resolution at the sample of approximately 1μm.Following the protocols established by previous studies of live and fixed cells [6, 12, 18, 28], the water immersion environment reduces the risk of photothermal damage of the cells by acting as a heat sink [29]. The confocal hole was set at 100μm. The instrument was spectrally calibrated to the 520 cm 1line of silicon. Correction of the intensity response function was performed using the Standard Reference Material (SRM) No. 2243 of the US National Institute of Standards, Boulder, Colorado (NIST SRM 2243, 2242, 2241) [3]. A 300 lines/mm grating was used, providing a spectral dispersion of approximately 1.5 cm^{-1} per pixel (6.16 cm^{-1} full width half maximum of the source 785 nm laser line). The spectral range of the fingerprint region, from 400 cm^{-1} to1800 cm^{-1} was captured in a single spectral window.

For the Raman spectroscopy measurements, the co-culture models were prepared and irradiated as described in sections 2.3 and 2.5. All experiments were performed in triplicates, such that each irradiation time point (30, 60, 90, 120 and 180 min) is represented by three control plates and three individual Petri dish samples. Raman microspectroscopic analysis was performed for both the first group, immediately after irradiation and the second, incubated for 24 h post-exposure. After SSR exposure, the PBS was exchanged for pre-warmed DMEM/F12 (phenol red free) medium for the Raman spectroscopic analysis of the samples. The samples were measured en-face, and ten keratinocytes, visible on the surface, were selected to acquire single

Raman spectra for each co-culture skin model, focusing on their nuclei to specifically elucidate DNA damage as a result of SSR exposure. The backscattered Raman signal was integrated for 30 s and accumulated twice to improve the signal-to-noise ratio. 30 spectra were collected from both irradiated and control samples, which were then subjected to pre-processing (baseline correction and smoothing) to improve the quality of the acquired spectra for further analysis.

2.9 Data analysis

For the AB assay for each time point, three independent experiments were conducted. Test results for control samples were set at 100%, and those for each time point were expressed as percentage of the control +/- standard deviation (SD).

Raman spectral data were pre-processed before analysis to remove the spectral background using Matlab 2017(Mathworks). The Extended Multivariate Signal Correction (EMSC) protocol, previously reported for baseline correction and background signal removal [19, 30, 31]was employed throughout. The EMSC algorithm adapted from Kerr et al. [31], also described in detail in Lopez-Gonzalez et al. [12] is used in this work to remove the background signal originating from the collagen I rat-tail and Geltrex extracellular matrices employed to produce the co-culture model. As reference spectrum the average spectrum of the sample data was employed.

The mean spectrum, recorded directly from the ECM immersed in DMEM/F12 medium (phenol red free) represents the spectral contribution of ECM. The slowly varying baseline is represented by an appropriate N^{th} order polynomial. N=3 was chosen as the most appropriate polynomial order, correcting the baseline and removing the ECM contribution from the spectra. The corrected spectra were subsequently smoothed using the Savitzky–Golay method (polynomial order of 5 and window 13) to improve spectral quality. No significant contributions from the underlying glass to the recorded spectra was observed, and thus, no correction was

deemed necessary.

Raman spectra were subjected to principal components analysis (PCA) and partial least squared regression (PLSR), combined with 10-fold cross-validation, to analyse the spectral variation in the co-culture model. PCA aims to reduce the number of variables in a multidimensional data set (i.e. spectra) [32], keeping most of the variance within the data set. PCA is a multivariate technique which analyses the data set by reducing multiple variables to a small number of a significant linear combination (Principal components). In PCA, two new set of axes, called principal components (PC), are generated by forming linear combinations of the original axes. The first PC is the linear combination containing the maximal variance contained within the data; PC2 is the subsequent linear combination which has maximal variance perpendicular to the first PC, and so on. As part of the PCA, two new matrices are generated, called scores and loadings, from which the variability within a dataset, as well as the spectral origins can be visualised. PLSR is a technique which constructs a linear model which associates variations in the spectral data to a target dataset. [26,33] In this work, the targets are the times of irradiation (e.g. 30 min, 60 min, 90 min, 120 min and 180 min) and the values of the AB assay response (% cell viability). The predictive models were developed using a 10-fold cross validation approach. [34] The optimal number of latent variables for the calibration model was determined using the goodness of fit R^2 value and the mean squared error of prediction (MSEP), 10 fold in cross validation.

PCA score plots show whether spectra collected from irradiated cells at different time points can be differentiated, whereas the PC loadings identify spectral features which are changing due to the action of simulated of solar radiation on cells. Although the PLSR methodology is commonly employed to build models to predict the cellular response based on their spectroscopic profiles, [26,33] in this work, the regression co-efficients are analysed to identify the direct effects of radiation on the nuclei of cells as a function of (i) duration of radiation

exposure and (ii) the cytotoxicological response as registered by the AB assay. One-way ANOVA of the PC scores was employed to verify the significance of differences between groups. A P value was considered to be statistically significant if it was less than 0.05.

3 RESULTS AND DISCUSSION

3.1 Light microscopy imaging

The co-cultured model was constructed to assess the SSR damage to keratinocytes cells in a 3D environment and the biochemical differences between 2D and 3D cultures were compared. The organisation of the model consists of a bottom layer composed of HDF embedded in collagen I coated with an upper layer of Geltrex where keratinocytes are seeded to be on top of the co-culture. The co-culture forms a gelatinous mass in the center of the Petri dish of 20 mm (glass diameter) as presented in Figure 1a. The surface of the model is completely covered by keratinocytes on the 13th day and it can then be used to undertake the radiation studies. Histological assessment of cross-sectional samples of 10 µm thickness was achieved using standard H&E staining. Hematoxylin, a positively charged basic dye, stains cell nuclei in blue, whereas eosin, a negatively charged acidic dye, stains the ECM and most cellular organelles in pink. [35] Figure 1 shows the spatial arrangement of HaCaT cells in co-culture with HDF in a 3D model. The double-layer of HaCaT cells grown over the ECM is clearly visible, with large nuclei stained in dark-blue and the cytoplasm in pink colour. Similar to HaCaT cells, the nuclear compartments of the less dense HDF (red arrow) cells are stained dark blue and their elongated cytoplasm is stained in pink, as shown in Figure 1c,d. A consistency of 2 to 3 layers of keratinocytes growing on top of each other was observed across different samples.

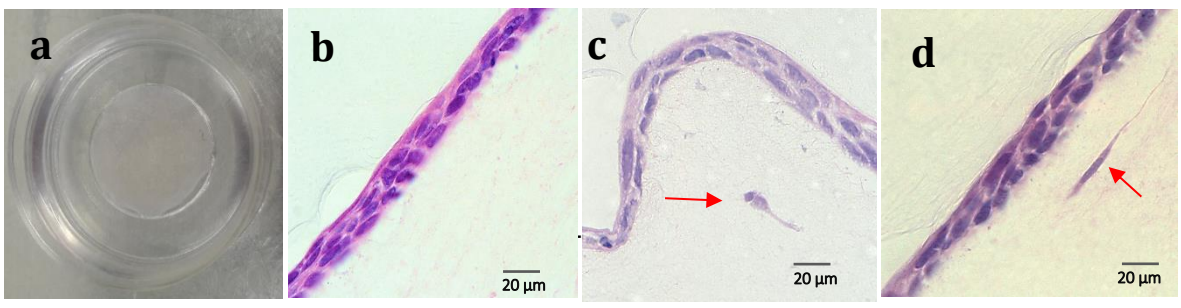

Figure 1. Microscopic examination of the H&E stained co-culture model. The morphology of fibroblast and keratinocytes is similar to that in normal human skin.

3.2 Cell viability measurement with Alamar Blue

The viability levels of HaCaT and HDF cells in a 3D matrix were evaluated with the commonly used AB cytotoxicity assay. Resazurin, the active ingredient in the AB assay, is reduced to resorufin, due to the cellular respiration metabolic reactions.[7], [22]

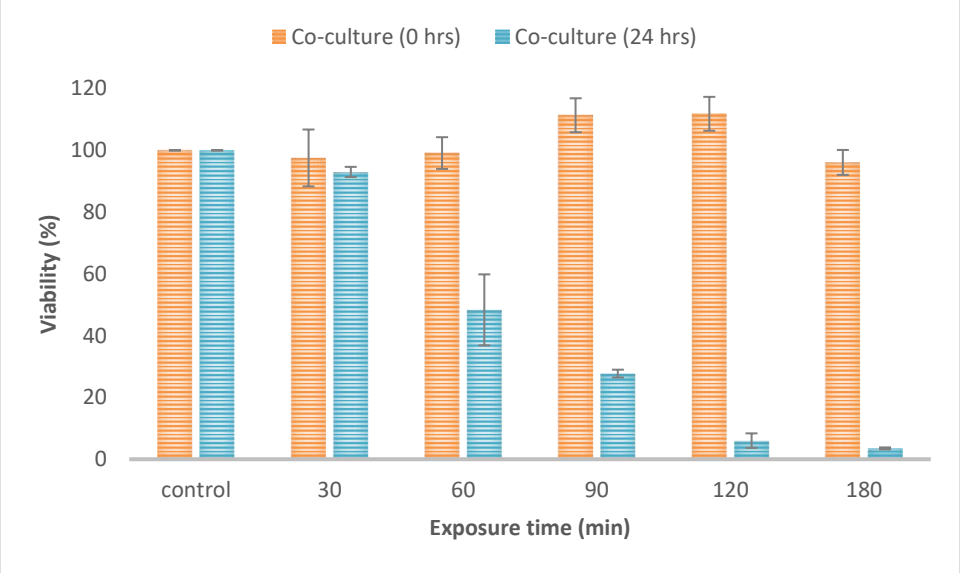

Figure 2. Alamar Blue response of the co-culture model to solar radiation for varying exposure times analysed immediately and 24 h post exposure.

This change from oxidised to reduced state allows a quantification of the effects of SSR on the 3D cell culture model via fluorometric detection.[11] Figure 2 displays the AB fluorescence measured immediately and 24 hrs post exposure for the co-culture model. When measured immediately after irradiation, no systematic reduction in the viability of the cell population, compared to control, is observed. When analysed 24hrs after irradiation, however, the AB

fluorescence intensity, compared to control, is observed to decrease monotonically. After 60 min of cell exposure, the cell viability value has reduced by more than 50%.

3.3 Raman analysis

Raman microspectroscopic analysis was used to acquire molecular information regarding the mechanisms of action of the SSR on HaCaT cells in co-culture with HDF cells. Raman spectroscopy elucidates a detailed spectroscopic profile of the cells and monitors the biochemical response in a time dependent manner. Thirty-point spectra per time of exposure (e.g. 30, 60, 90, 120 and 180 min) including control were acquired, specifically focusing on the nuclei of HaCaT cells seeded on the top of the co-culture models. The spectra were averaged for each time of exposure, and are shown in Supplementary Figure S1. Literature derived, typical band assignments of cellular spectral features employed in further analysis are detailed in Table 1. [11], [18], [19], [30], [31] Notably, any differences between the spectra of the SSR exposed cells are not striking, and therefore PCA was employed in an attempt to elucidate more subtle changes.

Table 1 [11], [18], [19], [30]–[31]

Raman band (cm^{-1})	**Assignment**
600	Nucleotide conformation
625	Glutathione
675	Glutathione
680	Ring breathing modes in the DNA bases.
716-18	A
750	T, DNA bases
766	Pyrimidine ring breathing mode
790-4	O-P-O phosphodiester bands in DNA
813	Distinct peak for RNA (together with 1240 cm^{-1})
839	Amide III, Tyrosine
850	B-DNA
870-4	Ribose vibration, one of the distinct RNA modes (with 874 and 918 cm^{-1})

893	Phosphodiester, Deoxyribose
918	Ribose, distinct mode of RNA
926	C-C aminoacids
951	Protein alfa helix
974	Ribose, distinct mode of RNA
981	C-C stretching in proteins
994	C-O ribose, C-C
1004-6	Phenylalanine, C-C skeletal
1036	Phenylalanine
1047	Carbohydrates
1080	Phosphodiester groups in nucleic acids
1093-97	Symmetric PO_2^- stretching vibration of the DNA backbone-phosphate backbone
1179	Cytosine, Guanine
1210	C-C stretch backbone carbon phenyl ring
1238-40	RNA
1251	A (ring breathing modes of the DNA/RNA bases)
1280	Nucleic acids and phosphates
1323	G (B, Z marker)
1338	G
1375	T,A,G (ring breathing mode DNA/RNA)
1400	CH_2
1417	Deoxyribose, (B,Z-marker)
1438	CH def, proteins, lipids
1480	G, A (DNA, RNA)
1492	DNA
1507	A (ring breathing mode)
1515-20	C
1583	-N-H bending vibrations of G, A residues within DNA/Phnylalanine
1605-08	Phenylalanine
1626-30	Amide C=O stretching
1640	Amide I
1655	Amide I
1672-77	Amide I (β-sheet)

Immediately after irradiation, PCA of all the data display some degree of clustering, although, there is no clear trend on which to base a loadings analysis (supplementary Figure S2). A pairwise analysis was therefore performed, comparing control with each time of exposure. [32] Figure 3 presents the scores plots (a) comparing control (green) versus exposed cells (blue) analysed immediately after irradiation. Although varying but limited degrees of clustering and

differentiation are observed for the shorter exposure times, the spectra corresponding to control and 180 min are clearly differentiated by PC1 (explained variance 42%), on the basis of their biochemical features. Using ANOVA of the PC scores, significant differences are indicated for control vs 30 min (P = 0.0018); 120 min (P = 0.0486) and 180 min ($P = 1.324 \times 10^{-13}$), although not for control vs 60 min (P = 0.0772) and 90 min (P =0.410). The loading of PC1 for control vs 180 min (Figure 3b), which shows the spectral features relevant for the discrimination, highlights positive peaks related to exposed cells, whereas negative to control.

(a)

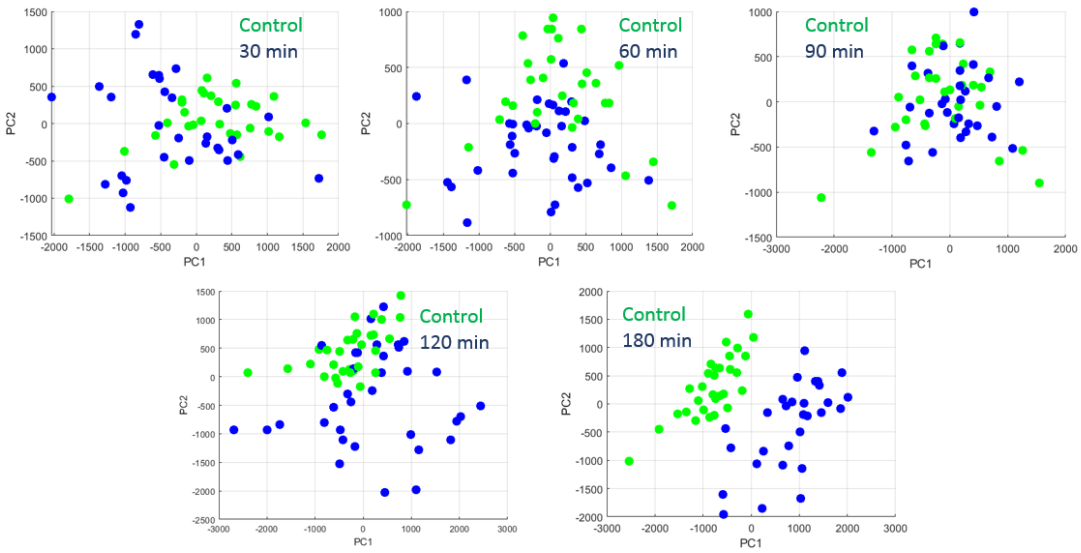

(b)

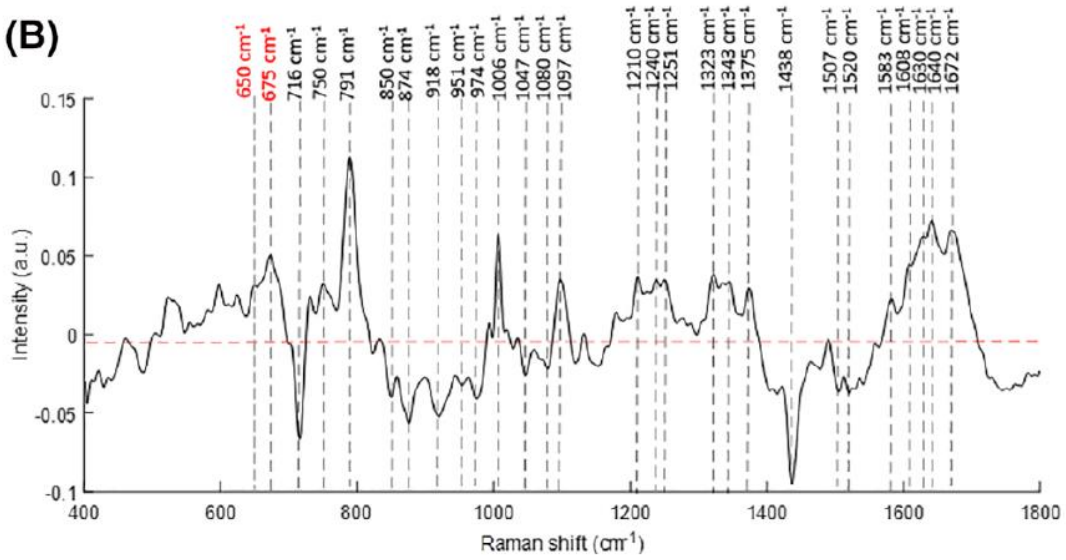

Figure 3 PCA scatter plots (a) and first loadings (b) derived from comparison of control and irradiated cells (180 min). ANOVA indicates significant differences for control vs 30 min (P = 0.0018); 120 min (P = 0.0486) and 180 min (P = 1.324×10^{-13}), although not for control vs 60 min (P = 0.0772) and 90 min (P =0.410).

The PC1 loading is mainly dominated by positive contributions of nucleic acids (750 cm^{-1}, 791 cm^{-1}, 1097 cm^{-1}, 1240 cm^{-1}, 1251 cm^{-1}, 1323 cm^{-1}, 1343 cm^{-1}, 1375 cm^{-1} and 1583cm^{-1}), proteins (1006 cm^{-1}, 1210 cm^{-1}, 1608 cm^{-1}, 1630 cm^{-1}, 1640 cm^{-1} and 1672 cm^{-1}) and peptides (625cm^{-1} and 675 cm^{-1}). The prominent bands identifiable in the negative loadings are due to nucleic acids 716 cm^{-1}, 850 cm^{-1}, 874 cm^{-1}, 918 cm^{-1}, 974 cm^{-1}, 1080 cm^{-1}, 1507 cm^{-1} and 1520 cm^{-1}) and proteins (951 cm^{-1} and 1438 cm^{-1}).

(a)

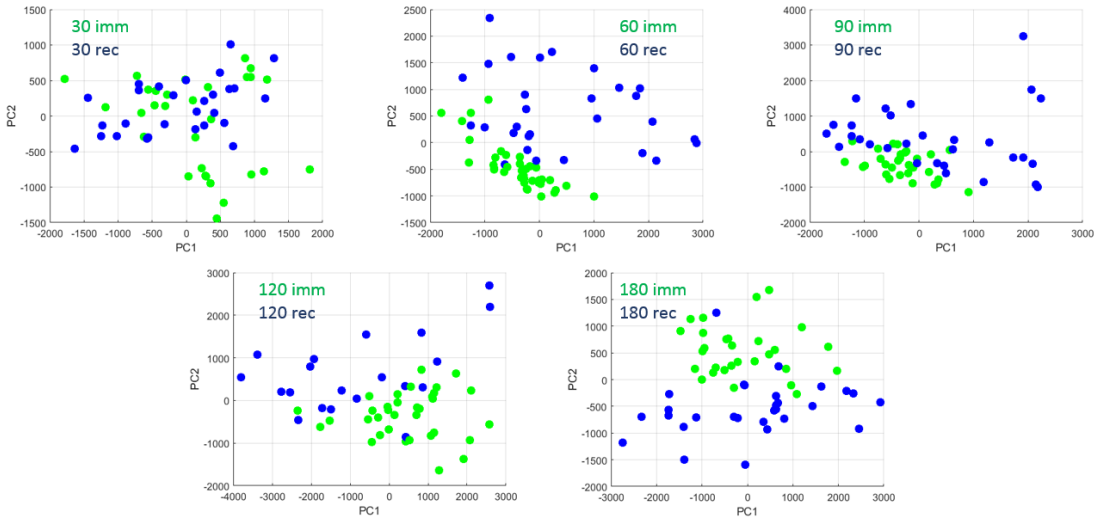

(b)

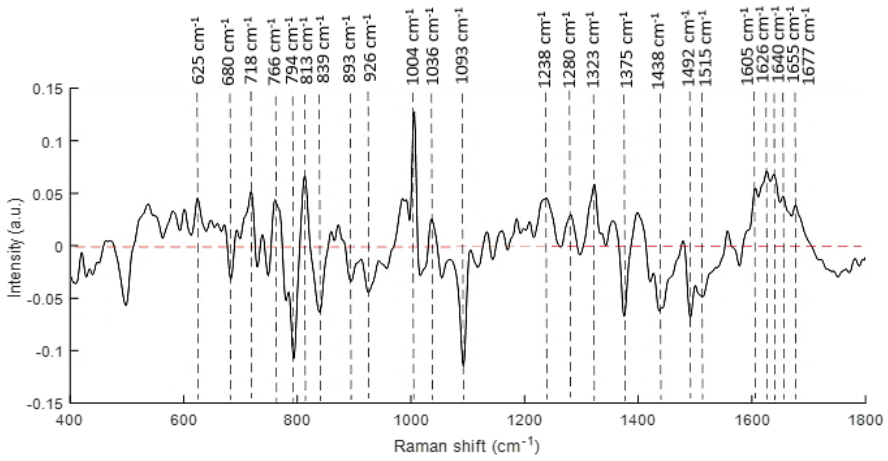

Figure 4 PCA scatter plots (a) and second loadings (b) derived from comparison of cells analysed immediately (180 min) and 24 hrs post exposure (180 min). ANOVA indicates significant differences for control vs 60 min ($P = 1.921 \times 10^{-11}$); vs 90 min ($P = 5.125 \times 10^{-5}$), 120 min ($P = 6.672 \times 10^{-9}$) and 180 min ($P = 3.622 \times 10^{-13}$), but not for control vs 30 ($P = 0.059$).

Raman spectra of cells which were analysed immediately and 24 hrs post exposure, for each exposure time, were subjected to PCA to elucidate biochemical relevant information concerning the influence of the irradiation on the metabolism of the cell. Figure 4 presents the score plots (a) comparing these two groups and the second PC loadings (b). In contrast to the PCA analysis of the results immediately post irradiation (Figure 3), the cluster separation is observed to be

primarily according to PC2 (explained variance 16%), whereas PC1, accounts for the most variance in the data set (45%), and describes the diversity of the groups due to intra-sample variability of the sampled points. Significant differences were indicated for control vs 60 min ($P = 1.921 \times 10^{-11}$); vs 90 min ($P = 5.125 \times 10^{-5}$), 120 min ($P = 6.672 \times 10^{-9}$) and 180 min ($P = 3.622 \times 10^{-13}$), but not for control vs 30 ($P = 0.059$).

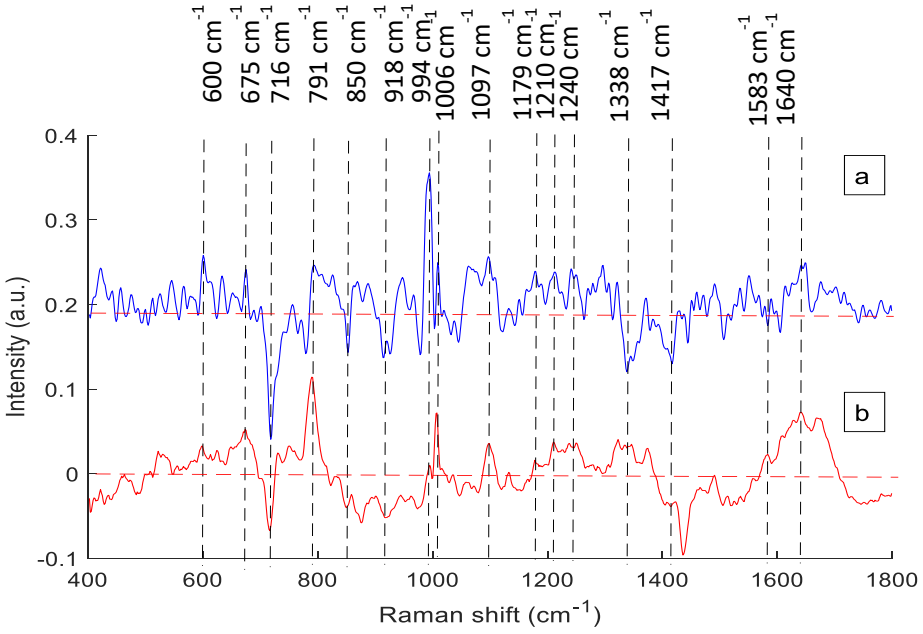

Figure 5 Partial least squared regression (PLSR) of Raman spectra of cells analysed immediately after irradiation against exposure time. Exposure time regression co-efficient (a) and principal component loading (b) of control versus 180 min. The horizontal red dashed lines represent the zero point of PC1 and PLSR co-efficient. The black vertical dashed lines highlight regions of conformational and biochemical changes due to the action of simulated solar radiation in cells.

The positive features in the PC2 loading are related to spectra of cells exposed for 180 min (immediate) and are associated with nucleic acids (718 cm^{-1}, 766 cm^{-1}, 813 cm^{-1}, 1238 cm^{-1}, 1280 cm^{-1} and 1323 cm^{-1}), and proteins (1004 cm^{-1}, 1036 cm^{-1}, 1605 cm^{-1}, 1626 cm^{-1}, 1640 cm^{-1}, 1655 cm^{-1} and 1677 cm^{-1}). Negative features related to 180 min (24 hrs post exposure) are derived from nucleic acids (680 cm^{-1}, 794 cm^{-1}, 893 cm^{-1}, 1093 cm^{-1}, 1375 cm^{-1}, 1492 cm^{-1} and 1515 cm^{-1}) and proteins (839 cm^{-1} and 1438 cm^{-1}). (Table 1).

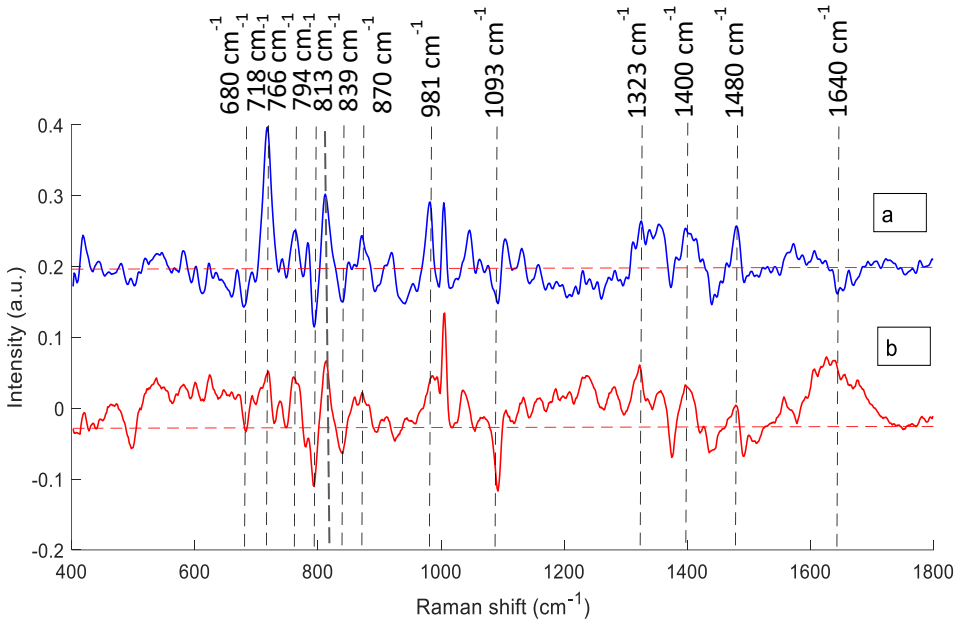

Figure 6 Partial least squared regression (PLSR) against cell viability for Raman spectra of cells analysed 24 hrs after irradiation. Regression co-efficient against exposure time (a) and PCA loading (b) of 180 min immediate versus 180 min 24 hrs post exposure. The horizontal red dashed lines represent the zero point of PC1 and PLSR co-efficient. The black vertical dashed lines in the spectra highlight the regions of conformational and biochemical changes due to the action of simulated solar radiation in cells.

PLSR of the Raman spectra against the target of (a) exposure time, immediately after irradiation was used to identify signatures of direct radiation damage. Regression against (b) the AB cell viability 24 hrs post exposure was explored to identify signatures of later cellular response. The number of components selected to fit the model in (a) were obtained from the MSEP plot, which is presented in Figure S3 of supplementary material. 5 components were found to account for 89% of the variance. The model provides a linear trend of regression with a correlation accuracy (R^2) of 0.89 (Figure S4a). The regression coefficient plot presented in Figure 5 is compared with the PC1 loading of Figure 3(b). The spectral features show increases (positive bands) or decreases (negative bands) in the intensity of a specific vibrational response, due to changes in the biomolecular content, conformation or morphology. [33] Negative spectral features related mainly to nucleic acids (716 cm^{-1}, 850 cm^{-1}, 918 cm^{-1}, 1179 cm^{-1}, 1338 cm^{-1} and 1417 cm^{-1}) are

also present as negative features in the PC1 loading, which characterise control cells. Positive spectral features, derived from nucleic acids (600 cm^{-1}, 791 cm^{-1}, 974 cm^{-1}, 1097 cm^{-1} and 1240 cm^{-1}) and proteins (1210 cm^{-1} and 1640 cm^{-1}) are present in the PC1 loading as spectral features of irradiated cells.

Raman spectra of cells analysed 24 hrs post exposure were also subected to PLSR using the target of cell viability to obtain information regarding metabolic changes within cells. Although the MSEP plot (Figure S3b) suggests that 75% of the variance is accounted for by 3 - 4 components, 5 were selected to fit the model. The model yielded a correlation accuracy (R^2) of 0.81 thus providing a better linear prediction (Figure S4b). Figure 6 shows the regression co-efficient plot, which also displays the PC2 loading of Figure 4. The positive spectral features in the PLSR are related to decreased cell viability and are also associated to those bands in PCA loading coming from spectra of cells analysed 180 min immediately after irradiation. The positive bands are associated to nucleic acids (680 cm^{-1}, 718 cm^{-1}, 766 cm^{-1},813 cm^{-1}, 874 cm^{-1}, 1323 cm^{-1} and 1480 cm^{-1}) and proteins (981 cm^{-1}). Features of the negative side of the PLSR are derived from nucleic acids (680 cm^{-1}, 794 cm^{-1} and 1093 cm^{-1}) and proteins (1640 cm^{-1}). (Table1). The Raman data concerning spectra of cells analysed 24 hrs post exposure was also regressed against time of exposure. Figure S5b (supplementary material) presents the regression co-efficient, which, although inverted, is almost identical to that of the regression against viability.

3.4 Discussion

In this study, the results of using HaCaT, kerotinocytes, co-cultured with HDF, fibroblast cells, embedded in a 3D extracellular matrix, as a simplistic 3D in vitro model of skin, and the impact of SSR on the cells, as monitored using a conventional cytotoxicity assay and Raman microspectroscopic analysis, are reported. The two commercial products, collagen I and Geltrex, provided the cells with a 3D culture microenvironment to grow and proliferate, [6] as

depicted in Figure 1. The HaCaT cells attached rapidly to the surface of the co-culture, forming confluent layers (2 to 3) within 13 days, and have the capacity to differentiate, as reported in previous studies.[34] It is noted that several types of similar and more sophisticated artificial skin models which mimic human skin tissue have been successfully reconstructed in vitro.[10], [28], [35] These approaches can represent a multi-layered epithelium, from dermis, mainly composed of collagen fibres, to the stratified epidermal layer. Such models are less than ideal, however, and have been demonstrated to be limited in their barrier function, for example, determined by lipid packing in the stratum corneum.[9] Moreover, commercially available models are delivered full differentiated, and it is therefore not possible to investigate the effects of external insults such as SSR on the evolution processes. Rather than develop a stratified epidermis, the aim of this work was to elucidate the effect of the 3D environment of a simplistic co-culture model on the biochemical changes in HaCaT cells induced by SSR, in comparison to those previously observed in 2D cultures of these cells under the same conditions.[11]

A striking effect of the translation from 2D culture to 3D culture can be observed in the cell viability results assessed by the colorimetric cytotoxicity assay, AB. The results suggest that cells in a 3D environment, analysed immediately after irradiation, were not affected by the SSR with increasing time. This is in contrast to the observations for cells cultured in a 2D environment, which were seen to exhibit a clear monotonic reduction of viability levels due to exposure under the same conditions.[11] When analysed 24 hrs post exposure, a clear exposure time dependent reduction of culture viability was observed, and this more pronounced reduction of viability post exposure is similar to that observed in studies of 2D cultures, [11] as well as in artificial skin models [28] exposed to time dependent solar radiation. It should be noted, however, that the differences in the observed responses may be related to the performance of the AB assay in different cell culture environments.[6], [15] The effective surface area of each cell is different in the different culture environments, and the absorptive nature of the ECM can reduce the bioavailability of the assay dye, reducing the uptake rate. [6], [7] The results of the

conventional cytotoxicity assay in the two environments are therefore not directly comparable. Notably, the difference in the half maximal effective concentrations (EC_{50}) for 2D (0.66 Jcm^{-2}) [11] and 3D (0.45 Jcm^{-2}) models 24 hrs post irradiation is consistent with a dilution factor of 25%, previously observed in collagen matrices. [7] Accounting for such factors, therefore, the results suggest that there is little or no difference in cell viability response to SSR in both 2D and 3D cell cultures (24 hrs post exposure).

Significant differences have been reported, however,between the cycle of cells in 2D and 3D culture environ-ments [21, 41]. Gargotti et al. showed that cells culturedin 2D (CaF2substrates) manifest higher cell number inthe G0/G1 phase and fewer in the G2/M and S andphases, compared to those cells cultured in 3D (collagenmatrices) [6]. Notably, cell cycle can also be affected bySSR exposure, and, in turn, the sensitivity of cells to radi-ation exposure has been demonstrated [12]. Sandra et al.demonstrated that low levels of exposure to UV radiationare not likely to produce DNA strand breaks, but cellcycle arrest in the G2 phase, due to the induction of highlevels of the p16 protein, whereas levels of the p53 pro-tein are enhanced after high doses of UV. An apoptoticrather than cell cycle response is implicated [39, 41]. Theobservations suggests that the translation from 2D to 3Denvironments not only affects cell cycle but also cellinteractions with their surroundings. Moreover, otherstudies [42] suggest that cell morphology and geometry isalso modified in this transition.

As conventional cytotoxicity assays do not enable adirect comparison of 2D and 3D cultures, the ability ofRaman microspectroscopy to investigate the molecularalterations in the nucleus of cells by an external insult bySSR insult was explored. Raman microspectroscopic anal-ysis enables a direct analysis of the biochemical alter-ations in HaCaT cells due to SSR impact in the 3D modelsystem, which can be directly compared to thoseobserved in a 2D culture [12, 32]. Raman spectroscopicanalysis provided clear signatures of the characteristicbiochemical content of the nuclei of the cells. Notably,no strong background, attributable to auto-fluorescenceemission was observed, although it has been demon-strated that such emission, at

lower excitation wave-lengths of 640 nm, can be used to analyse oxidativeeffects of UV radiation [43]. The spectroscopic signaturesrelated to SSR impact on cell nuclei are not clearly dis-cernible in a plot of the averaged Raman spectra acquiredfrom the nucleus of cells analysed immediately, or24 hours post exposure (Figure S1), and therefore, Ramanspectra were subjected to the multivariate statistical tech-niques of PCA, to better visualise differences betweenexposed and non-exposed groups, and PLSR, to identifyprogressive spectral variations which are correlated withexposure time and cell viability.

According to the PCA of figure 3, immediately after exposure, spectra of cells irradiated for 180 min were clearly differentiated from those of control cells. PLSR also indicates that these differentiating features are progressive over the period of SSR, consistent with the observations of the AB assay. The spectral features of both the PC loading and regression co-efficient are associated with DNA backbone moieties (1097 cm^{-1}) and C-O ribose (994cm^{-1}), which suggests possible alterations to the main chain conformation of the DNA.[11] The co-efficient of regression against exposure time exhibits negative features related to nucleic acids (716 cm^{-1}, 850 cm^{-1} and 1338 cm^{-1}), ribose and deoxyribose structures (918cm^{-1} and 1417cm^{-1}) which suffered direct damage upon exposure, while positive features associated to DNA (791cm^{-1} and 1097cm^{-1}) and phenylalanine structure (1006 cm^{-1} and 1210 cm^{-1}) indicate modifications in these biological constituents. The bands related to ring breathing vibrations of phenylalanine (1006 cm^{-1} and 1210 cm^{-1}) and bending vibrations of guanine or adenine residues of DNA (1583 cm^{-1}) have been reported to be markers for UVR induced apoptosis in cells. [37] The bands assigned to glutathione (625 cm^{-1} and 675 cm^{-1}), corresponding to cells analysed immediately after irradiation, are considered a protective cell response to oxidative stress generated by UVR.[38]. All these observations can suggest induction of single strand breaks, formation of bipyrimidine photoproducts and oxidative damage of bases, as a direct effect of SSR on cells. [11], [37], [38]

To further investigate the biological mechanisms response to SSR exposure, the spectral profiles of cells analysed immediately and 24 hrs post exposure were compared using PCA and PLSR. Figure 6 shows Raman signals attributed to O-P-O stretching vibrations in DNA (794 cm^{-1}) and DNA backbone (1093 cm^{-1}). These bands can be correlated with internucleosomal DNA fragmentation in apoptotic cells. [11], [39], [40] In addition, the appearance of two bands at 791 cm^{-1} and 813 cm^{-1} may be related to non-coding RNA formation due to the ROS formation. [18] Associated with the disintegration of the DNA strands, a decrease in the protein content as presented in the negative bands associated with amide III (839 cm^{-1}) and amide I (1640 cm^{-1}) in the regression co-efficient can suggest activation of the caspase cascade in apoptotic cells. [39]

These observations are consistent with those previ-ously reported for 2D models and artificial skin models,in which DNA damage is mainly seen, immediately afterirradiation, as an early stage of cytotoxicity and proteindamage is mostly seen, 24 hours after irradiation, as alate response to radiation [12, 32]. Apart from the similarities between the two cell culture systems, there are signatures which were only identified in spectra of HaCaT cells cultured in 3D models. The bands located at 625 cm^{-1} and 675 cm^{-1}, associated with an immediate cellular response to UVR insult [33], are absent in spectra of HaCaT cells cultured in 2D models. It has been reported that nuclear glutathione possess antioxidant properties which protects the DNA and DNA-binding proteins from external insults as ionising radiation. [41] However, it is also implicated in the reduction of the nuclear environment as cells passes from G1 to G2/M phases to prevent DNA damage upon breakdown of the nuclear membrane which is affected during solar radiation exposure. [41], [42] The absence of these two bands in 2D models can be attributed to an altered cell response to drugs, compounds or external stimuli (UVR) due to their unnatural microenvironment. [4], [43], [44] In contrast, cells cultured in a 3D environment acquire a spatial arrangement which better reproduces in vivo-like conditions which favours

cellular responses to external stimuli and cellular functions such as proliferation, differentiation, gene and protein expression. [4]

4 CONCLUSION

In this work, the effects of culturing HaCaT cells in a 3D microenvironment on the impact of SSR are evaluated. The combination of two commercial products for 3D culture showed the potential to reproduce a viable microenvironment for cell growth and proliferation. This 3D in vitro model served to study replicative cellular functions mimicking in vivo-like skin responses to SSR. Although the conventional cytotoxicity assay indicated a significant difference between the cellular responses in 3D compared to 2D culture environments, the assay responses cannot be directly compared, due to the differing bioavailability of the dye. Raman microspectroscopy provides more direct evidence of the similarities in cellular response, as well as the differences, which may derive from enhanced cellular protection mechanisms associated with the antioxidant glutathione. Thus, coupled with multivariate statistical analysis, Raman microspectroscopy has been demonstrated to be an ideal tool to investigate molecular changes in the nuclear compartment of HaCaT cells irradiated with SSR. Apart from cell cycle, the spectral analysis showed that the cellular response to SSR is modified when cells are transferring from 2D to 3D environments.

ACKNOWLEDGMENTS

Ulises Lopez-Gonzalez was funded by Consejo Nacional de Ciencias y Tecnologia (CONACYT), Mexico.

AUTHOR CONTRIBUTIONS

Ulises Lopez-Gonzalez performed all experiments, analysis and drafting of the manuscript. Alan Casey advised on the experimental protocol. Hugh J. Byrne contributed to drafting of the manuscript.

CONFLICT OF INTEREST

The authors declare no potential conflict of interest

DATA AVAILABILITY STATEMENT

The data that support the findings of this study are available from the corresponding author upon reasonable request.

REFERENCES

[1] Duval, K., Grover, H., Han., Mou, Y., Pegoraron, A. F., Fredberg, J., & Chen, Z, In *Physiology.* **2017**, 32(4), 266–277.

[2] Hoarau-Véchot, J., Rafii, A., Touboul, C., & Pasquier, J. *Int. J. Mol. Sci.* **2018**, 19(1), 181.

[3] Charwat, V., Schütze, K., Holnthoner, W., Lavrentieva, A., Gangnus, R., Hofbauer, P., Hoffmann, C., Angres, B., & Kasper, C. *J. Biotechnol.* ***2015***, 205, 70–81.

[4] Lee, J., Cuddihy, M. J., & Kotov, N. A, *Tissue Engineering - Part B: Reviews*. **2008**, 14(1), 61–86.

[5] Rodríguez-Hernández1, C. O., Torres-García, S. E., Olvera-Sandoval, C., Ramírez-Castillo, F. Y., Muro, A. L., Avelar-Gonzalez, F. J., & Guerrero-Barrera, A. L, *Int. J. Curr. Res. Acad. Rev.* **2014**, 2(12), 188-200.

[6] Gargotti, M., Lopez-Gonzalez, U., Byrne, H. J., & Casey, A., *Cytotechnology*. **2018**, 70(1), 261–273.

[7] Bonnier, F., Keating, M. E., Wróbel, T. P., Majzner, K., Baranska, M., Garcia-Munoz, A., Blanco, A., & Byrne, H. J., *Toxicol. Vitr.* **2015.** 29(1), 124–131.

[8] Ivers, L. P., Cummings, B., Owolabi, F., Welzel, K., Klinger, R., Saitoh, S., O'Connor, D., Fujita, Y., Scholz, D., & Itasaki, N., *Cancer Cell Int.* **2014,** 14(1), 108.

[9] Tfayli, A., Bonnier, F., Farhane, Z., Libong, D., Byrne, H. J., & Baillet-Guffroy, A. *Experimental dermatology*. **2014**, *23*(6), 441-443.

[10] Tfayli, A., Piot, O., Draux, F., Pitre, F., & Manfait, M., *Biopolymers*. **2007**, 87(4), 261–274.

[11] U. Lopez-Gonzalez, A. Casey, and H. J. Byrne., *J. Biophotonics*. **2020**, e202000337.

[12] Maguire, A., Lyng, F. M., & Walsh, J. E., *Radiat. Prot. Dosimetry*. **2010**, 140(2), 147–157.

[13] Svobodová, A., & Vostálová, J. *Int. J. Radiat. Biol.* **2010**, 86, 999–1030.

[14] Tang, Y. L., & Guo, Z. Y. *Acta Biochim. Biophys. Sin. (Shanghai).* **2005,** 37(1). 39–46.

[15] Bonnier, F., Meade, A. D., Merzha, S., Knief, P., Bhattacharya, K., Lyng, F. M., & Byrne, H. J. *Analyst*. **2010**, 135(7), 1697–1703

[16] Meade, A. D., Byrne, H. J., & Lyng, F. M., *Mutat. Res.* **2010**, 704(1–3), 108–114.

[17] Short, K. W., Carpenter, S., Freyer, J. P., & Mourant, J. R., *Biophys. J.* **2005**, 88(6), 4274–4288.

[18] Gargotti, M., Efeoglu, E., Byrne, H. J., & Casey, A. *Anal. Bioanal. Chem.* **2018,** 410(28), 7537–7550

[19] Byrne, H. J., Sockalingum, G. D., & Stone, N. *RSC Anal. Spectrosc. Ser.* **2010**, 11, 105–143.

[20] Maguire, A., Morrissey, B., Walsh, J. E., & Lyng, F. M. *International journal of radiation biology*. **2011**, *87*(1), 98-111.

[21] Vega-Avila, E., & Pugsley,. In *Proc West Pharmacol Soc*. **2011**, 54(54), 10-14.

[22] Rampersad, S. N. *Sensors*. **2012**, *12*(9), 12347-12360

[23] Zachari, M. A., Chondrou, P. S., Pouliliou, S. E., Mitrakas, A. G., Abatzoglou, I., Zois, C. E., & Koukourakis, M. I., *Dose-Response*. 2014, *12*(2), 13-024.

[24] Bonnier, F., Ali, S. M., Knief, P., Lambkin, H., Flynn, K., McDonagh, V., & Byrne, H. J., *Vibrational Spectroscopy*. 2012, 61, 124-132.

[25] Bonnier, F., Mehmood, A., Knief, P., Meade, A. D., Hornebeck, W., Lambkin, H., ... & Byrne, H. J. *Journal of Raman spectroscopy*, **2011**, *42*(5), 888-896.

[26] Bassan P, Kohler A, Martens H, Lee J, Byrne HJ, Dumas P, Gazi E, Brown M, Clarke N, Gardner P. Analyst. **2010**,135(2), 268-77.

[27] Kerr, L. T., & Hennelly, B. M., *Chemometrics and Intelligent Laboratory Systems.* **2016**, *158*, 61-68.

[28] Ali, S. M., Bonnier, F., Ptasinski, K., Lambkin, H., Flynn, K., Lyng, F. M., & Byrne, H. J. (2013)., *Analyst*. **2018**, *138*(14), 3946-3956.

[29] Chan, J. K. *International journal of surgical pathology*. **2014,** *22*(1), 12-32.

[30] Notingher, I., Verrier, S., Romanska, H., Bishop, A. E., Polak, J. M., & Hench, L. L. *Spectroscopy*. **2002** *16*(2), 43-51.

[31] Kuhar, N., Sil, S., Verma, T., & Umapathy., S. *RSC advances*. **2018**, *8*(46), 25888-25908.

[32] Bonnier, F., & Byrne, H. J., *Analyst*. **2012**, *137*(2), 322-332.

[33] Roman, M., Wrobel, T. P., Panek, A., Efeoglu, E., Wiltowska-Zuber, J., Paluszkiewicz, C., ... & Kwiatek, W. M., *Scientific reports*, **2019,** *9*(1), 1-13..

[34] Pleguezuelos, O., & Kapas, S., *British Journal of Dermatology*. **2006,** *154*(4), 602-608.

[35] Brohem, C. A., da Silva Cardeal, L. B., Tiago, M., Soengas, M. S., de Moraes Barros, S. B., & Maria-Engler, S. S. *Pigment cell & melanoma research*. **2011**, *24*(1), 35-50.

[36] Pavey, S., Russell, T., & Gabrielli, B., *Oncogene.***2001**, *20*(43), 6103-6110.

[37] Singh, S. P., Kang, S., Kang, J. W., So, P. T., Dasari, R. R., Yaqoob, Z., & Barman, I., *Scientific reports*. **2017**, *7*(1), 1-8.

[38] Panikkanvalappil, S. R., Hira, S. M., & El-Sayed, M. A., *Chemical science*

. **2016**, *7*(2), 1133-1141.

[39] Verrier, S., Notingher, I., Polak, J. M., & Hench, L. L., *Biopolymers: Original Research on Biomolecules*. **2004**, *74*(1-2), 157-162.

[40] Brauchle, E., Thude, S., Brucker, S. Y., & Schenke-Layland, K., *Scientific reports*. **2014**, *4*(1), 1-9.

[41] Markovic, J., García-Giménez, J. L., Gimeno, A., Viña, J., & Pallardó, F. V., *Free radical research*. **2010**, *44*(7), 721-733.

[42] Kulms, D., Pöppelmann, B., Yarosh, D., Luger, T. A., Krutmann, J., & Schwarz, T., *Proceedings of the National Academy of Sciences*, **1999**, *96*(14), 7974-7979.

[43] Edmondson, R., Broglie, J. J., Adcock, A. F., & Yang, L. *Assay and drug development technologies*. **2014**, *12*(4), 207-218.

[44] Langhans, S. A. *Frontiers in pharmacology*. **2018**, *9*, 6.

SUPPORTING INFORMATION

Additional supporting information is available in the online version of this article at the publisher's website or from the author.